Marine Geology 379 (2016) 39–51

Contents lists available at ScienceDirect

Marine Geology

journal homepage: www.elsevier.com/locate/margo

Quantitative analysis of Paratethys sea level change during the Messinian Salinity Crisis

Alba de la Vara [a,b,*], Christiaan G.C. van Baak [a], Alice Marzocchi [c], Arjen Grothe [a], Paul Th. Meijer [a]

[a] Department of Earth Sciences, Faculty of Geosciences, Utrecht University, Heidelberglaan 2, 3584 CS Utrecht, Netherlands
[b] Environmental Sciences Institute, University of Castilla-La Mancha, Avenida Carlos III s/n, CP 45071 Toledo, Spain
[c] School of Geographical Sciences and Cabot Institute, University of Bristol, University Road, BS8 1SS Bristol, UK

ARTICLE INFO

Article history:
Received 22 October 2015
Received in revised form 5 May 2016
Accepted 6 May 2016
Available online 7 May 2016

Keywords:
Late Miocene
Paratethys
Sea level fall
Black Sea
Caspian Sea
Messinian Salinity Crisis

ABSTRACT

At the time of the Messinian Salinity Crisis in the Mediterranean Sea (i.e., the Pontian stage of the Paratethys), the Paratethys sea level dropped also. Evidence found in the sedimentary record of the Black Sea and the Caspian Sea has been interpreted to indicate that a sea level fall occurred between 5.6 and 5.5 Ma. Estimates for the magnitude of this fall range between tens of meters to more than 1500 m. The purpose of this study is to provide quantitative insight into the sensitivity of the water level of the Black Sea and the Caspian Sea to the hydrologic budget, for a scenario in which the Paratethys is disconnected from the Mediterranean. Using a Late Miocene bathymetry based on a palaeographic map we quantify the fall in sea level, the mean salinity, and the time to reach equilibrium for a wide range of negative hydrologic budgets. By combining our results with (i) estimates calculated from a set of recent global Late Miocene climate simulations and (ii) reconstructed basin salinities, we are able to rule out a drop in sea level of the order of 1000 m in the Caspian Sea during this time period. In the Black Sea, however, such a large sea level fall cannot be fully discarded.

1. Introduction

Nearly land-locked basins, like the Mediterranean Sea or the Paratethys (the predecessor of the Black Sea and the Caspian Sea), are highly sensitive to changes in climate due to their limited connection with the oceans (Thunell et al., 1988). In the Late Miocene, the Mediterranean Sea experienced the Messinian Salinity Crisis (5.97–5.33 Ma; Krijgsman et al., 1999; Manzi et al., 2013). This extreme geological event is expressed in a sequence of thick evaporites that were deposited in the basin in response to tectonic and glacio-eustatic restriction of the connection with the ocean (e.g., Roveri et al., 2014a). The consensual view is that during the climax of the Messinian Salinity Crisis (from 5.61 to 5.55 Ma) the Mediterranean sea level dropped about 1500 m (e.g., Hsü et al., 1973; Clauzon et al., 1996, see also Christeleit et al., 2015). Such a sea level fall would have terminated the inflow of Mediterranean waters into the Paratethys, but the Paratethyan water level would not simply mimic the Mediterranean drop due to the presence of sill(s) (e.g., Clauzon et al., 2005, Popov et al., 2006). Instead, the sea level of the Paratethys would be controlled locally by the interplay of tectonics (i.e., sill depth) and climate (i.e., hydrologic budget) after disconnection from the Mediterranean (e.g., Krijgsman et al., 2010). With a negative hydrologic budget (i.e., evaporation dominating over freshwater input by precipitation and runoff), the Paratethys sea level would have dropped. Since the Paratethys comprised multiple basins (e.g., Rögl, 1999), a sea level drop below the depth of the channels within the Paratethys would have potentially fragmented the sea into a series of individual sub-basins (Fig. 1a). From 5.6 to 5.5 Ma, roughly coincident with the climax of the Messinian Salinity Crisis, certain sub-basins of the Paratethys such as the Black Sea and the Caspian Sea may indeed have experienced a drop in sea level (e.g., Hsü and Giovanoli, 1979; Popescu, 2006; Gillet et al., 2007; Krijgsman et al., 2010; Leever et al., 2010; Abdullayev et al., 2012; Munteanu et al., 2012). In Paratethys terminology, this sea level drop occurred during the Pontian regional stage (e.g., Popov et al., 2006). The amplitude of the fall in the Black Sea and the Caspian Sea is highly debated and estimates range from tens of meters to more than 1500 m.

In this paper, to provide a quantitative basis for the debate, we perform a model analysis to test the sensitivity of the Late Miocene Black and Caspian sea levels to the hydrologic budget in these basins. Here we do so for a scenario in which the Paratethys is not connected to the Mediterranean Sea. Using a late Messinian bathymetry based on the palaeogeographic map of Popov et al. (2004) we quantify (i) the drop in sea level, (ii) the resulting average basin salinity, and (iii) the time needed for the sea level and salinity to reach equilibrium. This is done for a wide range of negative hydrologic budgets. In our calculations the drop in sea level is determined by the balance between evaporation minus precipitation (E − P) and river discharge (R). We first focus on the entire Paratethys and then we study the Black Sea and

* Corresponding author at: Environmental Sciences Institute, University of Castilla-La Mancha, Avenida Carlos III s/n, CP 45071 Toledo, Spain.
E-mail address: alba.delavara@uclm.es (A. de la Vara).

http://dx.doi.org/10.1016/j.margeo.2016.05.002
0025-3227/

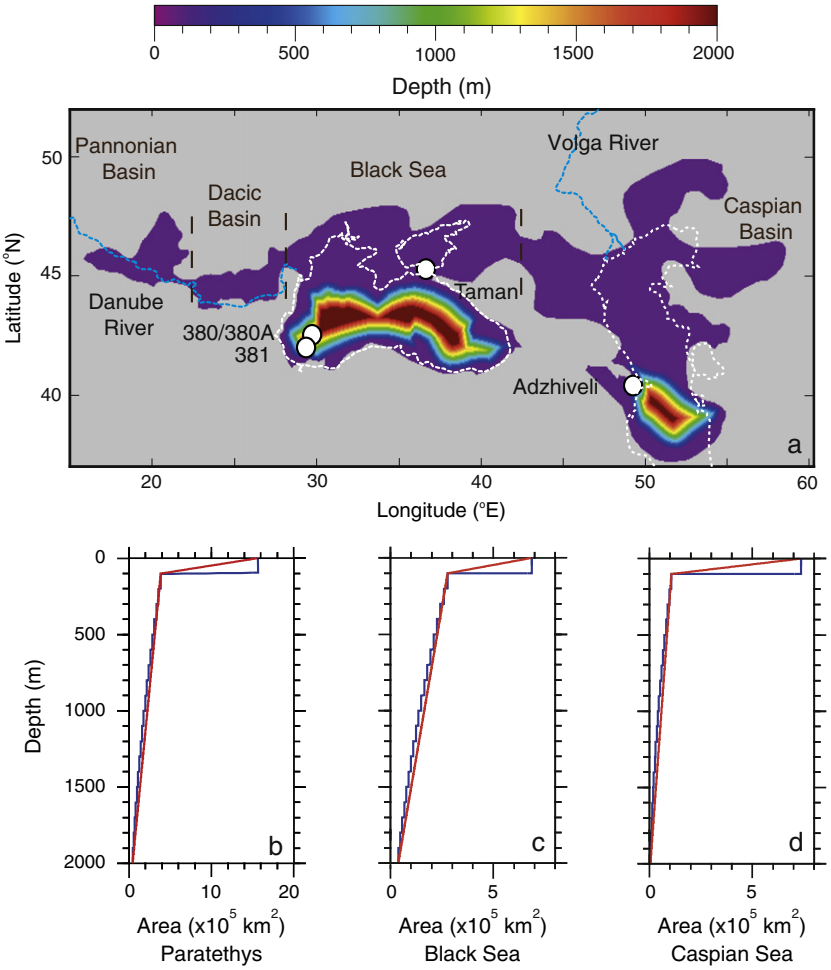

Fig. 1. Panel (a) shows the late Messinian bathymetry constructed from the palaeogeographic map of Popov et al. (2004). The circles show the location of DSDP sites 380/380A and 381, Taman Peninsula (Russia), and Adzhiveli (Azerbaijan). White dashed lines indicate the present-day coastline of the Black Sea and the Caspian Sea and the blue dashed lines the modern Danube and Volga rivers. Panels (b) to (d) show the hypsometric curves for the Paratethys, the Black Sea and the Caspian Sea, respectively. The blue hypsometric curves are built from the palaeobathymetry of panel (a). In the red curves a linear decrease of the surface area from the surface until 100 m, as well as from 100 m until 2000 m is assumed. Results shown in this paper are calculated with the red curves.

the Caspian Sea separately. Insight gained into the functioning of the Paratethys as a whole serves as a natural starting point and provides a reference for the case where the Black Sea and the Caspian Sea are treated as isolated basins. By using hydrologic budgets calculated for the Late Miocene Paratethys from the recent global climate model experiments of Marzocchi et al. (2015) and by comparing our results to salinity estimates inferred from geological data for this time interval, we aim to elucidate the magnitude of the sea level drop consistent with observations in the Black Sea and the Caspian Sea. In particular, we investigate whether a sea level drop of 1000 m or more is possible or not.

2. Regional setting

Throughout the Eocene-Oligocene, as a consequence of the incipient formation of the Alpine chains, a new marine realm separated to the north of the Tethys Ocean: the Paratethys (Rögl, 1999). This large epicontinental sea extended over Central and Eastern Europe and consisted of several sub-basins of which the Black, Caspian and Aral seas are the modern remnants. Later in time, during the Middle to Late Miocene, the progressive enclosure of the Paratethys gave rise to further differentiation between the Central Paratethys (Pannonian basin) and the Eastern Paratethys (Black Sea basin and Caspian basin; e.g., Rögl, 1996; see Fig. 1a). The Paratethys sub-basins were episodically connected through shallow channels (e.g., Kroonenberg et al., 2005; Popov et al., 2006) and sporadic Mediterranean-Paratethys connections have been documented (e.g., Popov et al., 2006; Suc et al., 2011; Vasiliev et al., 2013).

During the Deep Sea Drilling Project Leg 42b in the Black Sea, two boreholes (380 A and 381) revealed a presumed shallow-water stromatolitic dolomite unit, the so-called "Pebbly Breccia", at modern water depths deeper than 1700 m (see location in Fig. 1a; Ross et al., 1978). Based on tentative biostratigraphic studies it was concluded that the Pebbly Breccia had a Late Miocene age (e.g., Gheorghian, 1978; Jousé and Mukhina, 1978). However, in the 1970s age control on the Paratethys record was poor and the age assigned to this unit was questioned (Kojumdgieva, 1979). This notwithstanding, Hsü and Giovanoli (1979) proposed that the unit formed in response to a 1600 m amplitude sea level fall in the Black Sea coeval with the Messinian Salinity Crisis. Further studies correlated erosional surfaces observed in seismic profiles from the Black Sea to the Messinian Salinity Crisis, supporting the hypothesis that a sea level drop larger than 1500 m occurred during the Late Miocene (e.g., Gillet et al., 2003, 2007; Munteanu et al., 2012).

On the basis of new seismic surveys in the southwestern Black Sea, Tari et al. (2015) conclude that the Pebbly Breccia is an allochthonous mass-wasting event, as proposed earlier by Radionova and Golovina (2011); Alekseev et al. (2012) and Grothe et al. (2014). In recent

years, biostratigraphic and magnetostratigraphic studies have led to greatly improved age control on the Paratethyan successions (e.g., Vasiliev et al., 2005; Stoica et al., 2013) and recently it has been shown that the Pebbly Breccia is, at least, older than the Messinian Salinity Crisis (Grothe et al., 2014). In addition, lithological and faunal evidence from the Taman peninsula (Fig. 1a) has been interpreted to indicate a sea level drop of 50–100 m at 5.6 Ma (Krijgsman et al., 2010). However, the target section contains a hiatus at 5.6 Ma and the authors point out that their estimate must be considered a minimum. The seismic surveys of Tari et al. (2015) also show that the Late Miocene incisions over the Black Sea palaeoslope have a subaqueous origin. This, they argue, excludes the possibility of a sea level drop as large as 1600 m.

One of the main arguments to postulate a large sea level fall in the Caspian Sea is the presence of a deeply incising palaeo-Volga canyon through the Central Caspian Basin (Kroonenberg et al., 2005, Green et al., 2009; Abdullayev et al., 2012). This canyon has been interpreted to have formed in response to a base-level fall between 600 and 1500 m coeval with the Messinian Salinity Crisis (e.g., Jones and Simmons, 1996). However, the age of this canyon is poorly constrained. Other evidence in favour of a 1500 m sea level fall is the basinward shift of the depocenter observed in seismic profiles (Abdullayev et al., 2012). Similarly to the Black Sea, good age control has only been acquired lately. Using a cyclostratigraphic age model, van Baak et al. (in press) argue for a sea level drop of 100–150 m in Adzhiveli section (southwestern Caspian Sea; see location in Fig. 1a) between 5.6 and 5.5 Ma, in contrast with previous estimates.

3. Model setup

3.1. Underlying equations

In this analysis the rate of sea level (SL) drop in the basin studied (i.e., entire Paratethys, Black Sea, or Caspian Sea) is controlled by the surface freshwater flux (i.e., E − P) and the river discharge R (Eq. (1)). With SL for sea level in m, E − P in m/year, R in m^3/year, sea level dependent surface area A in m^2, and time t in years, the governing equations reads,

$$\frac{d}{dt}SL = (E-P) - \frac{R}{A(SL)} \quad (1)$$

Both E − P and R are assumed to be constant over time. The reduction of the surface area of the basin entailed by a drop in sea level increases the rate of the sea level rise due to river input. In all calculations E − P is greater than R/A at the outset. Sea level drop and salinity are calculated for the steady state, which is reached when the two terms on the right-hand side become equal.

To calculate the salinity associated with a certain sea level drop, the initial salt content of the basin is divided by the remaining water volume. Over time the salinity of the Paratethys waters varied between marine and fresh (e.g., Schrader, 1978; Popov et al., 2006). To account for this, each calculation is initialised with a range of salinities: 10, 20, or 35 g/kg. Empirical and theoretical studies have shown that evaporation decreases when the salinity of the body of water increases (e.g., Salhotra et al., 1985). We will consider the effect of salinity on the evaporation using the expression proposed in Topper and Meijer (2013). This consists of a linear fit to observational data regarding the evaporation rate as a function of salinity reported in Warren (2006). In our model setup we do not distinguish between evaporation and precipitation and, consequently, this parameterisation also affects precipitation (i.e., E − P). Following Topper and Meijer (2013), we assume this to be a valid approach given that other parameterisations are more complex and entail more assumptions. The resulting expression reads,

$$E-P = (E-P)_o \cdot 1.0316 \cdot \left(1 - 8.75 \cdot 10^{-4} \cdot S\right) \quad (2)$$

where S is salinity in g/kg and $(E - P)_o$ corresponds to the initial value of E − P before the sea level starts to drop. In each simulation E − P ranges from 0 to 3 m/year. R is varied between the values that would contribute a sea level rise from 0 to 3 m/year at the initial sea level, i.e. before any fall in level has occurred. In the Mediterranean Sea, the modern value of E − P is 0.6 m/year (Mariotti et al., 2002) and model studies have yielded 1 m/year for the Late Miocene (Gladstone et al., 2007). Estimates of present-day E − P are 0.1 m/year in the Black Sea (Ünlülata et al., 1990) and 0.7 m/year in the Caspian Sea (Ozyavas et al., 2010). At present, the river runoff is 350 km^3/year (0.8 m/year) in the Black Sea (Ünlülata et al., 1990) and 301 km^3/year (0.8 m/year) in the Caspian Sea (Ozyavas et al., 2010). We therefore expect 0–3 m/year to cover, by far, the range of E − P and R of the Late Miocene Paratethys.

3.2. Bathymetry and hypsometry

The bathymetry used for the calculations is built from the late Messinian palaeogeographic map of Popov et al. (2004), from which a gridded bathymetry with a uniform horizontal resolution of 1/20° × 1/20° is created. The deep and shallow domains distinguished on the palaeogeographic map are set to 2000 m and 100 m, respectively (Fig. 1a). A smooth transition between these two domains is achieved by the implementation of a continental slope. This consists of a linear increase of the depth from the shelves to 2000 m. As in the present-day Black Sea and Caspian Sea, this slope is considered relatively steep and narrow (e.g., Staneva et al., 2001). Arguing that water depths greater than 1000 m only existed in the central depressions indicated on the map (Popov et al., 2006), the continental slope is inserted on the "deep side" of the outer edge of the shallow domains shown on the map (Fig. 1a). Next, the horizontal area as a function of depth is computed from the surface until the seafloor at a vertical spacing of one meter (blue hypsometric curve in Fig. 1b).

Because in the bathymetry the shelf is considered 100 m deep starting right at the coastline, the hypsometry starts abruptly. This was found to create numerical instabilities and to correct for this we assume a linear transition between the surface area at 0 m and that at 100 m. To account for a more gradual decrease of the surface area from the continental slope to the deepest basin, we also adopt a linear transition from the surface area at 100 m and that at 2000 m (red curve in Fig. 1b). Results presented in this paper are computed using the red hypsometric curve. We first focus on the entire Paratethys and, at a later stage, assuming that the gateways connecting the subbasins were shallow (e.g., Popov et al., 2006), we study the Black Sea and the Caspian Sea separately. The hypsometric curves for the Black Sea and the Caspian Sea are calculated following the same procedure as for the Paratethys (Fig. 1c and 1d). Volume as a function of depth (not shown) is calculated by integration of the red hypsometric curves.

3.3. Alternative parameterisations

To test the effect of other parameterisations we perform several additional experiments. We investigate the possibility that the river discharge increases progressively as the sea level drops due to the implied increase of the surface area of the drainage basins. In this case we assume that the river discharge is proportional to the surface area of the drainage basins, following Jauzein and Hubert (1984). When the sea level falls, the newly desiccated area is added to the drainage basin. The surface area of the drainage basins at normal sea level is derived from the global Late Miocene climate simulations by Marzocchi et al. (2015).

The palaeogeography used to construct the palaeobathymetry does not provide specific information regarding the depths of the different domains there distinguished, neither about the exact configuration of the continental slope. To account for the uncertainties as to the bathymetry, we explore the sensitivity of results to bathymetric changes in the basins. To this end, we set the shelves to 250 m (instead of to 100 m). We also investigate the case where the continental slope is inserted on the shallow side of the shelf edge. Although this seems a less likely configuration, it does represent a useful alternative to test the robustness of our results. The corresponding hypsometries are presented in Fig. 2. In this figure hypsometric curves of the modern Black Sea and Caspian Sea are also presented for comparison to the Miocene ones. An important feature is that in the present-day Black Sea and Caspian Sea hypsometric curves the deep domains of the basin occupy a surface area that takes intermediate values between the Late Miocene curves. A summary of the surface areas and volumes calculated for the entire Paratethys, the Black Sea and the Caspian Sea is presented in Table 1.

4. Analysis and results

4.1. Reference experiments

The amplitude of the sea level drop, the associated salinity, and the time required to reach equilibrium in the entire Paratethys, Black Sea and Caspian Sea are shown in Figs. 3, 4, and 5. Since the river discharge corresponding to an equivalent rate of sea level rise which ranges from 0 to 3 m/year, is greater when the basin occupies a larger surface area, the maximum R considered is greatest in the Paratethys, followed by the Caspian Sea and the Black Sea (Table 1). In these experiments the basins are initialised with a salinity of 10, 20, or 35 g/kg and E − P is considered to be either dependent or independent of salinity.

Nearly the entire range of E − P and R tested results in a sea level fall smaller than 100 m (in Fig. 3 the purple colour dominates). For a specific basin, combinations of E − P and R with which the sea level drops below the shelves (i.e., below 100 m) are the same regardless of the initial salinity and E − P parameterisation. Comparing panels corresponding to the same basin, only subtle variations of the amplitude of the sea level drop appear when R is very small. When R is close to 0 km^3/year the sea level drops between 1500 and 2000 m depending on the initial salinity of the basin and the way in which E − P is defined. For a given basin, the base level fall is greater when E − P is not a function of salinity (e.g., Fig. 3a–d). When E − P is parameterised as a function of salinity, E − P decreases linearly as salinity increases and this reduces the magnitude of the sea level drop compared to when E − P is constant. For this reason, in this case, in a certain basin, the sea level drops less when the basin is initialised with a higher salinity (e.g., panels b–d). When E − P is independent of salinity the sea level drop remains the same regardless of the initial salinity prescribed.

For a given E − P, the absolute value of R required for a sea level drop below the shelves (i.e., larger than 100 m) is smaller in the Black Sea and the Caspian Sea individually than for the Paratethys as a whole (Fig. 3). Once the sea level drops below the shelves the surface area of the basins becomes substantially smaller (see Fig. 1 and Table 1). River discharge, which is assumed to be constant, is spread over a smaller area and contributes a greater sea level rise. When the horizontal surface area of the basin at levels deeper than the shelves is small, the balance between E − P and R will therefore be attained at higher positions of the sea level. When the Black Sea and the Caspian Sea are taken separately, the surface area below 100 m depth is smaller than when the entire Paratethys is considered. For this reason, the absolute value of R for which the sea level drops below the shelves is smaller for the Black Sea and the Caspian Sea individually. To achieve a sea level fall of 100 m or larger, a substantially smaller R is required for the Caspian

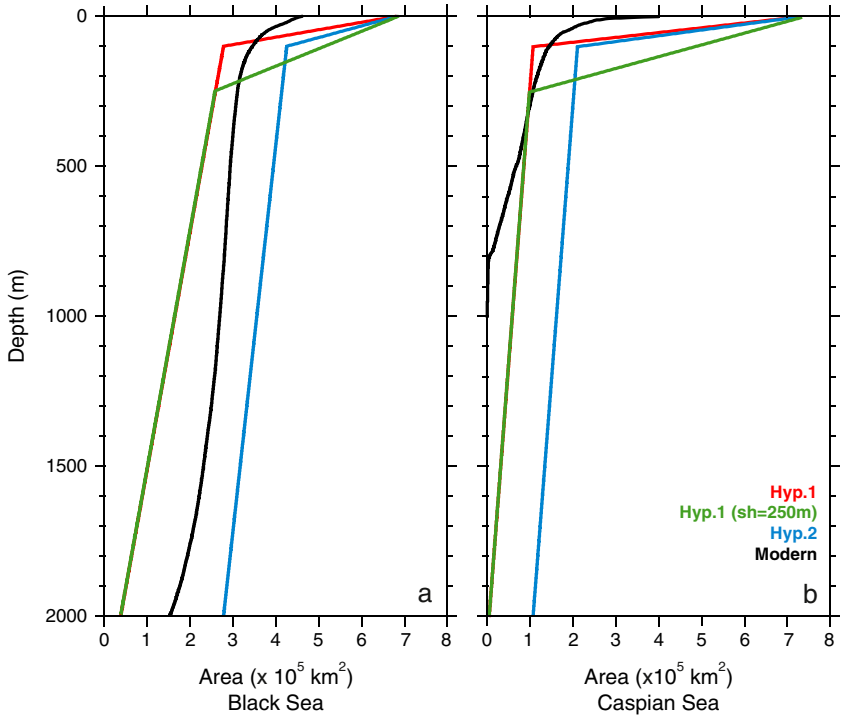

Fig. 2. Present-day (black lines) and Late Miocene (blue, red and green) hypsometries of the Black Sea (a) and the Caspian Sea (b). The red Late Miocene hypsometric curves are based on a bathymetry where the continental slope is introduced on the deep side of the shelf edge ("Hyp. 1"). The green curves differ from the red ones in that the shelves are set to 250 m (instead of 100 m; "Hyp. 1 (sh = 250 m.)"). The blue Late Miocene hypsometric curves are based on a bathymetry in which the continental slope is inserted on the shallow side of the shelf edge instead ("Hyp. 2"). Bathymetric data used to construct the present-day Black Sea and Caspian Sea hypsometries is extracted from the SRTM dataset (Farr and Kobrick, 2000) and the National Geographical Data Center of the NOAA, respectively.

Table 1
Summary of the surface areas and volumes of the Late Miocene Paratethys, Black Sea and Caspian Sea. Shallow domains correspond to the shelves (i.e., depth smaller or equal 100 m) and deep domains include all depths greater than that. Hypsometry 1 (Hyp. 1) is built from a bathymetry in which the continental slope is introduced on the deep side of the shelf edge. In hypsometry 2 (Hyp. 2) this is done on the shallow side.

		Total area ($\times 10^5$ km^2)	Area shallow domains ($\times 10^5$ km^2)	Area deep domains ($\times 10^5$ km^2)	Total volume ($\times 10^5$ km^3)	Volume shallow domains ($\times 10^5$ km^3)	Volume deep domains ($\times 10^5$ km^3)
Late Mioc. Parat.	Hyp. 1	15.6533	11.8057	3.8476	5.0485	0.9907	4.0578
	Hyp. 2	15.6533	9.2951	6.3582	10.8079	1.1162	9.6917
Late Mioc. Black Sea	Hyp. 1	6.8533	4.0751	2.7782	3.4872	0.4884	2.9988
	Hyp. 2	6.8533	2.6006	4.2527	7.2387	0.5621	6.6766
Late Mioc. Casp. Sea	Hyp. 1	7.3607	6.2913	1.0694	1.4878	0.4288	1.0590
	Hyp. 2	7.3607	5.2552	2.1055	3.4957	0.4807	3.0150

Sea than for the Black Sea because in the Caspian Sea the deep domains of the basin occupy a considerably smaller area (Fig. 1 and Table 1).

Salinity at equilibrium is shown in Fig. 4. Given that no gypsum or halite was deposited in the Black Sea and in the Caspian Sea during the Late Miocene, we set the upper limit of the colour scale to 150 g/kg for a better visualisation of results (i.e., the value at gypsum saturation). Salinities greater than 150 g/kg are shown in white. Salinity only starts to rise substantially relative to the initial salinity of the basin when the sea level is below the shelves. Although the shelves occupy a large surface area, the volume from the surface to the shelf depth is only a small part of the total volume of the basin and the salt contained in the shelves is small. In the Black Sea the shelves occupy 59% of the total area but the surface-to-shelf-depth volume only represents about 14% of the total volume. This is even more pronounced in the Caspian Sea, where

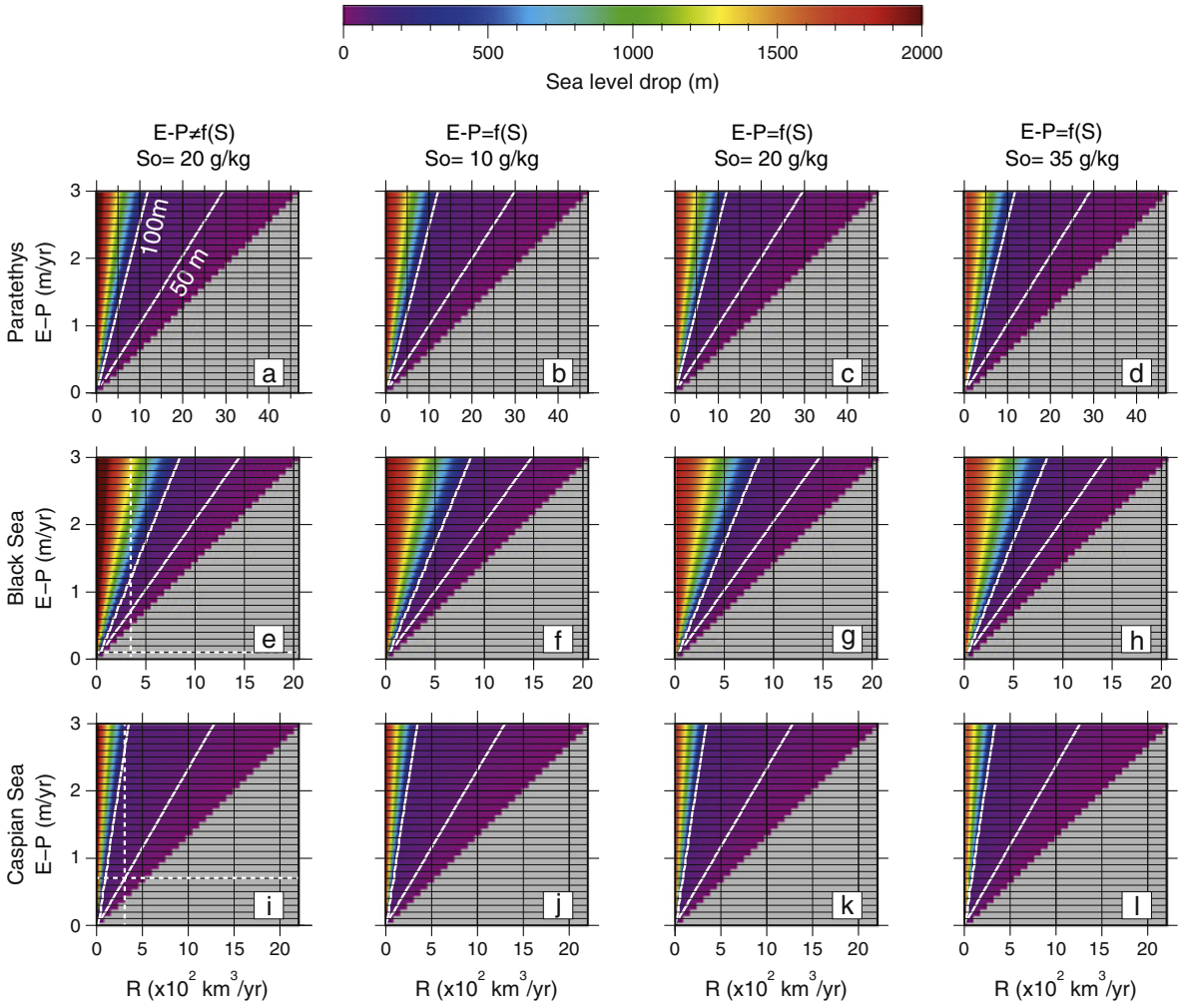

Fig. 3. Drop in sea level for the entire Paratethys (a–d), the Black Sea (e–h), and the Caspian Sea (i–l) for a wide range of hydrologic budgets. As indicated in the figure, in the first panel of each row of four, E − P does not depend on salinity and the basins are initialised with a salinity of 20 g/kg. In the next three panels, E − P is a function of salinity and the initial salinity of the basins is 10, 20, and 35 g/kg, respectively. White continuous lines indicate a sea level drop of 50 and 100 m. White dashed lines in panels (e) and (i) show the present-day hydrologic budgets of the Black Sea and the Caspian Sea, respectively. The Black Sea hydrologic budget derives from Ünlülata et al. (1990) and the Caspian Sea budget from Ozyavas et al. (2010). Grey areas denote regions where the hydrologic budget is positive.

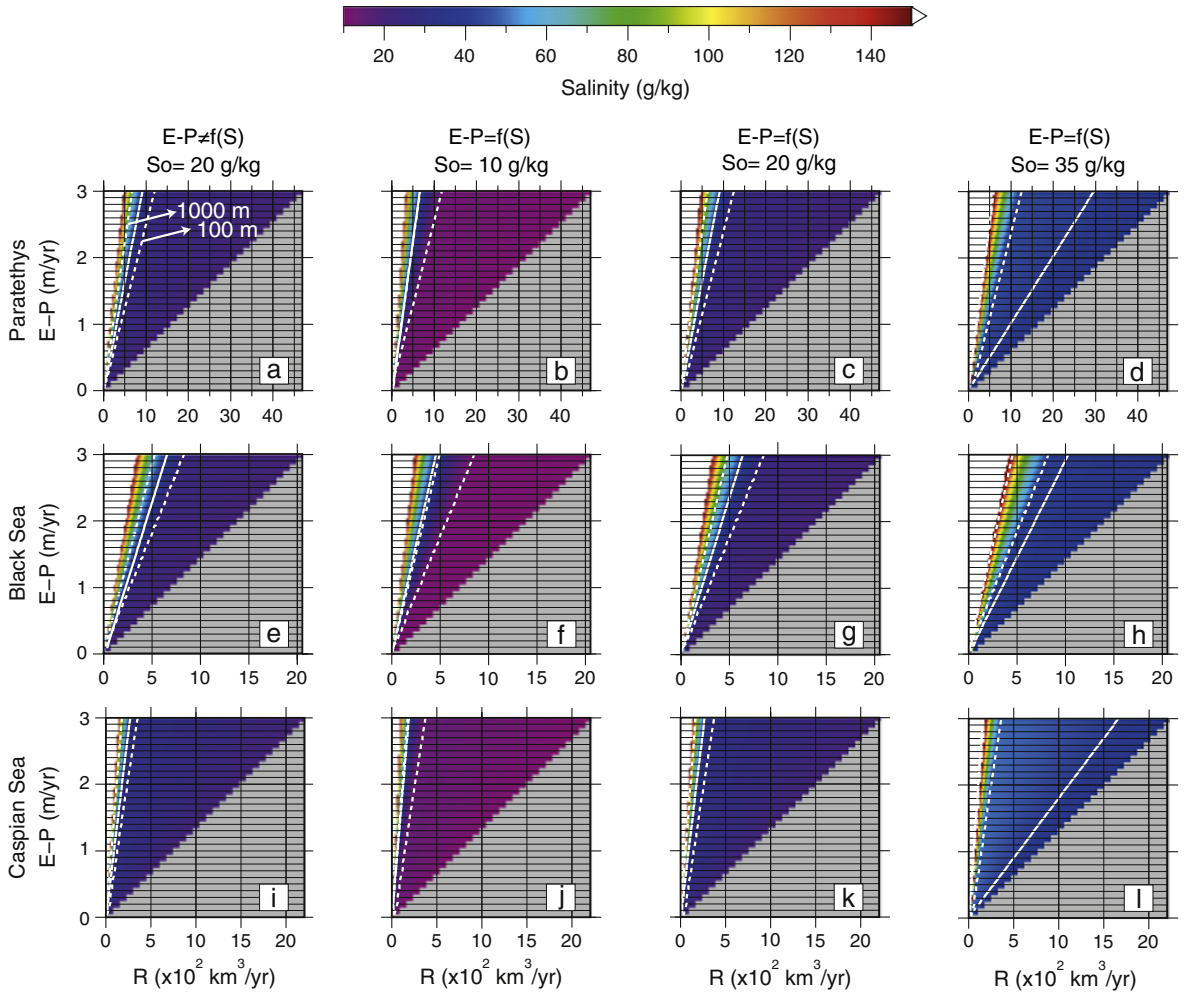

Fig. 4. Salinity at equilibrium in the Paratethys (a–d), Black Sea (e–h) and Caspian Sea (i–l) for a wide range of hydrologic budgets. In the first panel of each row of four, E − P is not dependent on salinity and initial salinity is 20 g/kg. In the next three panels E − P is a function of salinity and the basins are initialised with 10, 20, or 35 g/kg, respectively. White continuous lines indicate a salinity of 40 g/kg and white dashed lines show the hydrologic budgets that correspond to a 100 and 1000 m sea level drop, as indicated in panel (a). The areas coloured in grey correspond to positive hydrologic budgets. Note that in panels (b), (f) and (j) the contours showing the 1000 m sea level drop and 40 g/kg closely overlap.

the numbers are 85% and 29%, respectively. Once the sea level drops below the shelves the volume becomes substantially smaller in the Caspian Sea than in the Black Sea (Table 1). For a given sea level drop larger than the shelves, salinity would rise more in the Caspian Sea than in the Black Sea (e.g., see the 1000 m sea level drop contour of Fig. 4e–l).

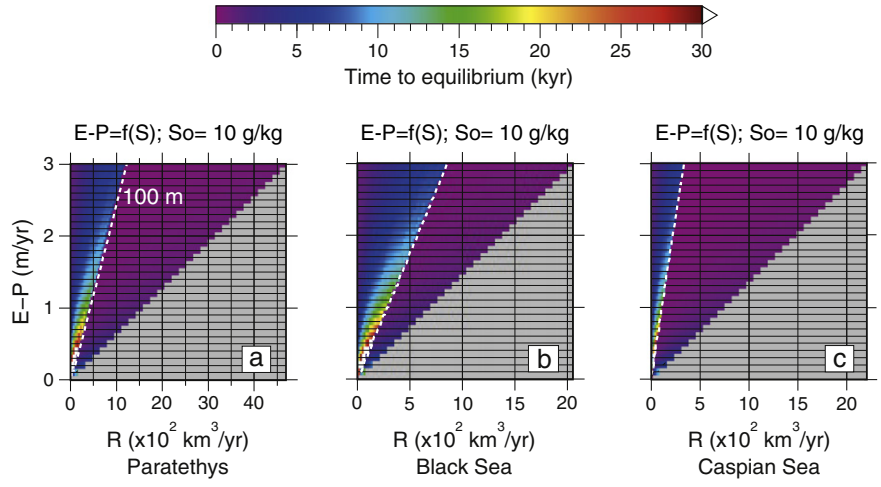

Fig. 5. Time to reach equilibrium in the Paratethys (a), Black Sea (panel b), and Caspian Sea (c). E − P is parameterised as a function of salinity and the basins are set to an initial salinity of 10 g/kg. The discontinuous lines correspond with the hydrologic budgets for which the sea level drops 100 m. The grey regions of the plot indicate positive hydrologic budgets.

Fig. 5 shows the time to equilibrium for the entire Paratethys, the Black Sea and the Caspian Sea. For a given basin, essentially no deviations due to different E − P parameterisation and initial salinity occur. For brevity we here focus on the case where E − P is a function of salinity and the basins are initialised with a salinity of 10 g/kg. Time to equilibrium never exceeds 80–90 kyr. We observe that for most of the hydrologic budgets tested a steady state is reached within 10 kyr. Time to equilibrium is shortest for sea level drops over the shelves (i.e., smaller than 100 m). In the areas adjacent to the boundary between a positive and a negative hydrologic budget time to equilibrium is short, but slightly longer for small values of E − P and R. Time to equilibrium is longest when the sea level drops below the shelves because this entails the evaporation of a greater volume of water which takes longer, especially for small fluxes of R and E − P.

4.2. Additional experiments: alternative parameterisations

Because it proves representative, we will examine the role of the other parameterisations only for the case where E − P is a function of salinity and the basins have an initial salinity of 10 g/kg. Results obtained with river discharge depending on drainage area are depicted in panels (a) to (c) of Fig. 6. Due to the increase in R, for a given E − P and starting value of R, the sea level falls less compared to the equivalent reference experiment (see Fig. 3b, 3f, 3j). For this reason a specific hydrologic budget also entails a smaller salinity (not shown). Time to equilibrium proves not to be significantly different (not shown).

The sea level drop in the whole Paratethys, Black Sea and Caspian Sea when the shelves are set to a maximum depth of 250 m is shown in Fig. 6d to f. Because we assume a linear decrease from the surface area at the surface to that at 250 m, shelves are deeper everywhere (see Fig. 2). Notwithstanding the greater depth of the shelves, the hydrologic budgets for which sea level drops below the shelves remain roughly unchanged compared to the equivalent reference experiment (cf. Fig. 3b, 3f, 3j). Comparing these results to equivalent experiments with shallow shelves we find that a specific hydrologic budget now entails a slightly higher salinity (not shown). Because shelves are deeper, hydrologic budgets that drop the sea level over the shelves entail a greater fall in sea level and therefore higher salinity. For hydrologic budgets that correspond to sea level drops below the shelves salinity is slightly greater due to the deeper nature of the shelves, which increases the salt content of the basin. For each basin, time to equilibrium for sea level drops over the shelves is somewhat longer than that in the reference experiments, but it never exceeds 10 kyr (not shown). For larger falls in sea level time to equilibrium is very similar to that in the reference experiments (not shown).

Finally, we consider the case that the slope is introduced on the shallow side of the outer edge of the deep domains. The sea level drop for the entire Paratethys, the Black Sea and the Caspian Sea is shown in Fig. 6g, 6h, and i, respectively. With this hypsometry, in a given basin

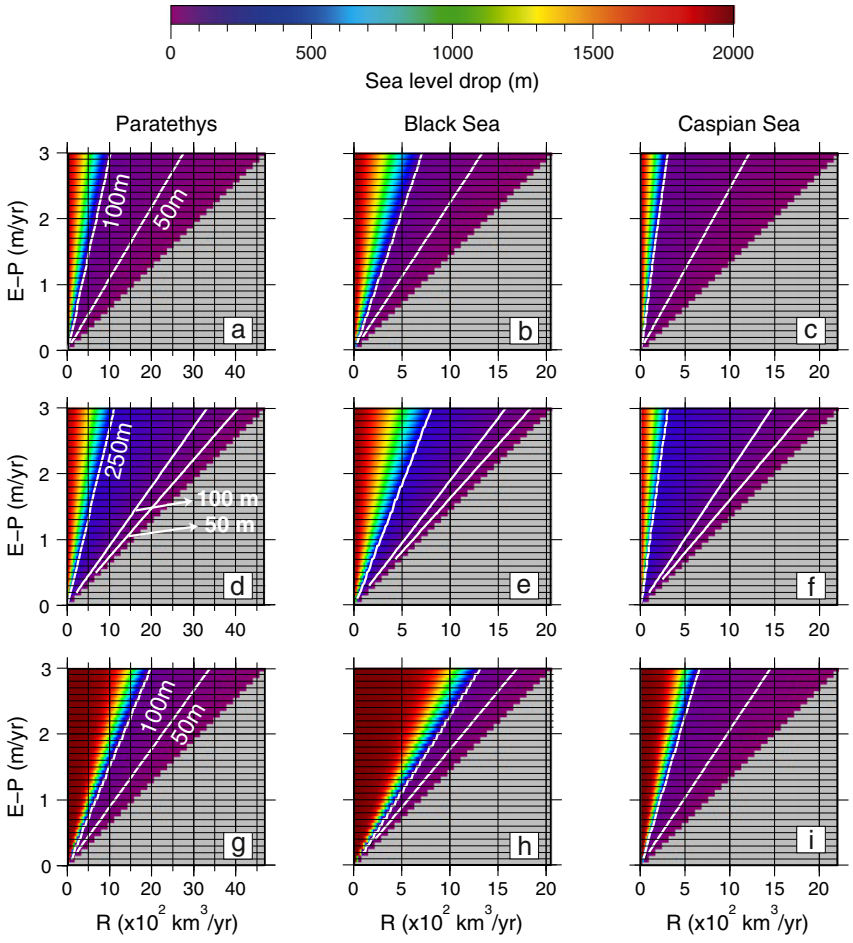

Fig. 6. Sea level drop in the Paratethys as a whole (a, d, g), Black Sea (b, e, h) and Caspian Sea (c, f, i) as a function of the hydrologic budget and for several alternative parameterisations. E − P is a function of salinity and initial salinity of the basins is 10 g/kg. In panels (a) to (c) the river discharge is proportional to the surface area of the drainage basins as proposed by Jauzein and Hubert (1984). In panels (d) to (f) the shelves are set to 250 m. In panels (g) to (i) the continental slope is inserted on the shallow side of the shelf edge. White contours indicate a sea level drop of the amplitude specified in the figure. Grey areas correspond to positive hydrologic budgets.

and for a specific hydrologic budget, the sea level stabilises at greater depth than in the previous experiments (see Fig. 3 and Fig. 6a to f). This is a direct consequence of the fact that the deep domains of the basin are now more extensive and the area for which R/A balances E − P is only found at greater depth (Fig. 6g–i). Because of this, the associated salinity is also higher (not shown). It takes a longer time to reach equilibrium than in the equivalent reference experiment, especially when E − P and R are small (not shown). However, time to equilibrium never exceeds 10 kyr for sea level drops over the shelves and 100 kyr for sea level drops below them (not shown).

5. Discussion

Summarising our model results, we find that, for a given hydrologic budget, a larger sea level drop occurs when the Paratethys is considered as single basin than when the Black Sea and the Caspian Sea are examined separately. In the latter case, for a specific hydrologic budget, a larger drop in sea level is attained in the Black Sea than in the Caspian Sea. To achieve a 1000 m sea level fall the hydrologic budgets of the basins have to be substantially different from the present-day values (Fig. 3). Important deviations from the initial salinity of the basin(s) are only found when large sea level drops occur (Fig. 4). Time to equilibrium is, for most of the hydrologic budgets tested, not longer than 10 kyr (Fig. 5). The alternative parameterisation that affects results to a larger extent is to insert the continental slope on the outer edge of the limit between the deep and shallow domains (Fig. 6). Also in this case the hydrologic budgets need to be substantially different from the modern ones to achieve a 1000 m sea level fall (Fig. 6). Below we use these results to discuss the outstanding geological issues. A summary of the assumptions made in the different experiments presented so far, is offered in Table S1 of the Supplementary data.

5.1. A large Late Miocene sea level drop in the Black Sea?

During the Late Pleistocene, as a result of lowered global sea level during glacial periods, the Black Sea repeatedly became isolated from the Mediterranean Sea (Badertscher et al., 2011). While this caused the Black sea level to go down (Zubakov, 1988), this however did not result in a sea level fall as large as 1000 m or in desiccation of the Black Sea. We will use our analysis to assess the likelihood of such a large sea level drop in the Black Sea during the Late Miocene. We will assume that the level of the Paratethys does not simply follow the falling level of the Mediterranean, in other words, that the two are separated by a sill located higher than the lowered Mediterranean water surface (e.g., Clauzon et al., 2005, Popov et al., 2006). Arguing that the connection between the Black Sea and the Caspian Sea was shallow (e.g., Popov et al., 2006), we determine the hydrologic budgets that would cause a 1000 m sea level drop in an isolated Black Sea. We take E − P to be not greater than 1 m/year, the value proposed for the Mediterranean Sea during the Messinian Crisis (Gladstone et al., 2007). To achieve a 1000 m sea level drop in the Black Sea, R has to be close to 0.23 m/year (i.e., 158 km^3/year) or smaller if E − P is less than 1 m/year (Fig. 7b). This value of R is about two times smaller than the modern river discharge into the Black Sea (350 km^3/year; Ünlülata et al., 1990) and is close to the present-day Danube River discharge (199 km^3/year; Garnier et al., 2002).

While these numbers perhaps already speak against a large-magnitude drop, it would clearly help to have a constraint on the

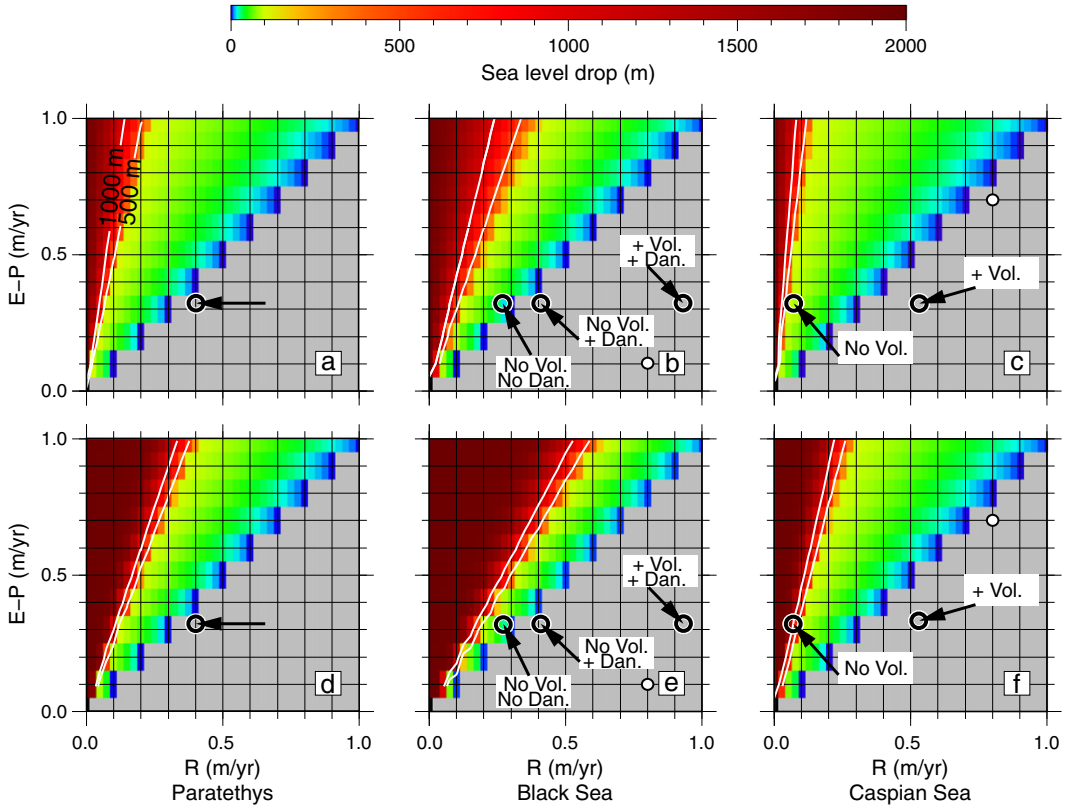

Fig. 7. Estimated sea level drop for the entire Paratethys (a and d), Black Sea (b and e), and Caspian Sea (c and f). Note that the x-axis is now expressed in (m/year). In all cases E − P is prescribed as a function of salinity and the basins are initialised with 10 g/kg. In (a) to (c), the hypsometry used for the calculations is built from a bathymetry where the continental slope is inserted on the deep side of the shelf edge. In panels (d) to (f), the hypsometry used for the calculations is constructed from a bathymetry where the continental slope is inserted on the shallow side of the shelf edge instead. The circles indicate the hydrologic budgets derived from the global climate simulations by Marzocchi et al. (2015). "Dan." and "Vol." refer to the Danube and Volga rivers, respectively. White lines approximate a sea level drop of 500 and 1000 m. White dots in panels (b–c) and (e–f) show the modern hydrologic budget of the Black Sea (Ünlülata et al., 1990) and the Caspian Sea (Ozyavas et al., 2010). Grey areas indicate positive hydrologic budgets.

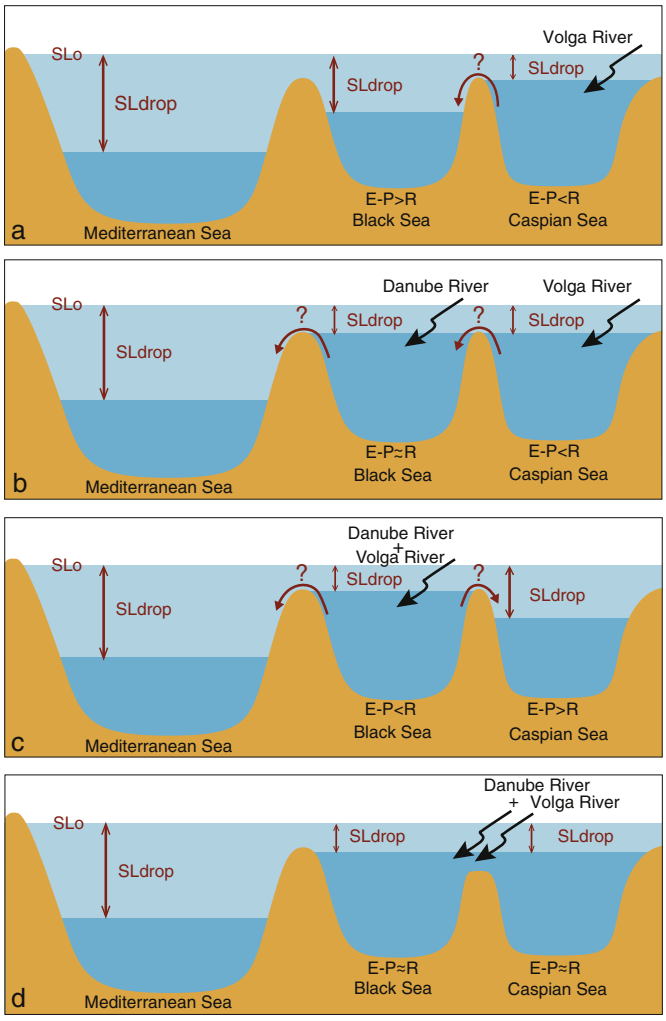

Fig. 8. Schematic illustration of the sea level configuration in the Black Sea and the Caspian Sea for different configurations of the sills between the basins and using the hydrologic budgets from Marzocchi et al. (2015). In panels (a) to (c) the sill between the Mediterranean Sea and the Paratethys (most likely via the Aegean region; Popov et al., 2006) has a similar depth to that between Black Sea and the Caspian Sea. Once the Mediterranean sea level falls below the connecting sill, the Black Sea and the Caspian Sea become separated basins and develop their own hydrologic budgets. In panel (d) the sill between the Black Sea and the Caspian Sea is deeper than that to the Mediterranean. A lowering of the Mediterranean sea level below the sill does not separate the Black Sea and the Caspian Sea and both basins would have the same hydrologic budget. Initial sea level is indicated as SLo. Arrows between basins indicate possible overspilling from a basin into another.

hydrologic budget at the time. For this we turn to Marzocchi et al. (2015), who performed experiments with a global ocean-atmosphere-vegetation coupled model for the Late Miocene. We calculated the annual mean hydrologic budget of the Paratethys averaged over the duration of the full Late Miocene precession cycle simulated by Marzocchi et al. (2015). The methodology, which is derived from Gladstone et al. (2007), and the hydrologic budgets calculated from the simulations of Marzocchi et al. (2015), are presented in the Supplementary data. We account for the fact that, since the configuration of the Late Miocene drainage system is uncertain (e.g., Gillet et al., 2007; Munteanu et al., 2012), there are different possibilities as to the location of discharge of the Danube and the Volga (Fig. 7 and see Fig. 8a–c also). Only when we assume that neither of these rivers entered the Black Sea, the hydrologic budget takes negative values (i.e., $E - P > R$; Fig. 7b). This would result in a sea level drop of about 30 m and corresponds to an equivalent freshwater flux ($E - P - R$) of 0.05 m/year, which is much smaller than that of the present day Mediterranean Sea (0.5 m/year). This indicates that even in the extreme case that none of the major rivers flowed into the Black Sea the hydrologic budget calculated from the simulations by Marzocchi et al. (2015) does not correspond to a 1000 m sea level drop. Although the uncertainty attached to the climate model-derived budgets is hard to quantify, our figures allow to directly judge the effect of a given variation around the values used here. The hydrologic budget when the Volga and the Danube rivers did not flow into the Black sea is only slightly negative and a large sea level drop would require extreme deviations from the calculated budget, certainly surpassing the model error. In agreement with this, the pollen record from the southwestern Black Sea (borehole 380A) of Popescu et al. (2010) combined with the updated age model of van Baak et al. (2015) indicates no large changes that would point to a shift towards an extremely dry environment. This contradicts, however, results inferred from hydrogen isotopes measured on alkenones ($\delta D_{alkenone}$) from the Black Sea. These suggest that dry conditions prevailed at the time and that the hydrologic budget for this period was strongly negative (Vasiliev et al., 2013, 2015). As an alternative explanation for the heavy $\delta D_{alkenones}$ signal, Vasiliev et al. (2013) propose that this could represent a Mediterranean signal transferred into the Paratethys by evaporation.

Another way to constrain past sea level changes is via the salinity of the basin waters (salinity will increase when the water volume decreases). Sea-surface salinity observations reported by Schrader (1978) in sites 380/380A and 381 have recently been dated by van Baak et al. (2015) using a new high-resolution age model. In borehole 380/380A one of the diatom species used to reconstruct surface salinity (*Coscinodiscus stokesianus*) shows an abrupt increase in abundance during the time interval of the Messinian crisis. The salinity preference of this species is unknown and this causes salinity estimates to be subject to large uncertainty. Van Baak et al. (2015) consider both the possibility that this species represents fresh-to-brackish conditions (as done in Schrader, 1978) and the case that it indicates a marine environment. Comparing the estimated values just prior to 5.6 Ma with the maxima inferred for the interval from 5.6 to 5.5 Ma, the first possibility considered by van Baak et al. (2015) yields a change from a salinity of 3 to maximally 23 g/kg. The second case gives a change from a salinity of 10 to, at the highest, 25 g/kg. Combined with our model calculations, these changes would correspond to a sea level fall of 1400 m and 785 m, respectively (Fig. 9). These values are clearly higher than those inferred from the climate model results. However, we must keep in mind that salinity reconstructions are uncertain to start with. In addition, whereas the diatoms provide us with an estimate of sea-surface salinity, our model considers basin-averaged values. Salinity at shallow depths is more prone to change in response to surface processes and, for that reason, may show more extreme salinity variation. The observed increase in salinity could alternatively be explained by the presence of a marine connection between the Mediterranean and the Paratethys, responsible for an incursion of seawater. Note, this scenario requires the Mediterranean sea level to have been high during the climax of the salinity crisis, which has been recently proposed (Roveri et al., 2014b).

How robust are the insights reached so far to alternative parameterisations? In Section 4.2 we find that when the river discharge increases gradually as the sea level drops, for a given basin and a hydrologic budget, the sea level falls slightly less than in the equivalent reference experiment (Fig. 3 and Fig. 6a–c). When the shelves are set to 250 m, a given combination of $E - P$ and R results in a slightly larger sea level drop over the shelves relative to the equivalent reference experiment. However, this does not affect the magnitude of sea level drops below the shelves (Fig. 3 and Fig. 6d–f). These alternative parameterisations thus do not affect much the preceding discussion. In contrast, when the alternative hypsometric curve is considered (blue curve in Fig. 2), a given hydrologic budget corresponds to a substantially greater sea level drop (Fig. 3 and Fig. 6g–i). In Fig. 7e we observe that when this hypsometry is used, the

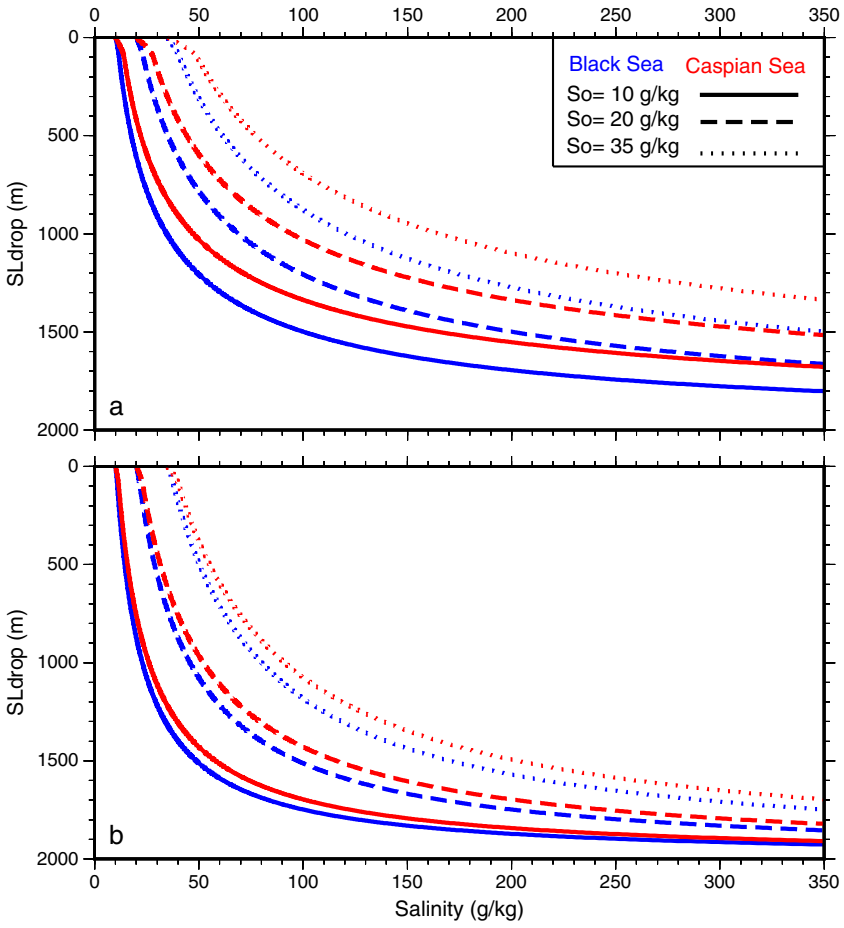

Fig. 9. Salinity (g/kg) as a function of the sea level drop (m) in the Black Sea (blue lines) and Caspian Sea (red lines) when the basins are isolated. The basins are initialised with a salinity (So) of 10 g/kg (solid lines), 20 g/kg (dashed lines) and 35 g/kg (dotted lines). The hypsometries used are built from either a bathymetry in which the continental slope is introduced on the deep (a) or the shallow sides (b) of the shelf edge.

Black Sea hydrologic budget derived from the simulations of Marzocchi et al. (2015) excluding the Danube and Volga rivers now results in a sea level drop of about 50 m. Surface salinity estimates from van Baak et al. (2015) correspond to a sea level drop of 1675 and 1080 m, respectively (see Fig. 9b). Thus, as found with the reference hypsometry, a 1000 m sea level drop is technically possible on the basis of salinity reconstructions, but it is not supported by the calculations based on the climate simulations of Marzocchi et al. (2015).

To summarise, the sea level drop calculated on the basis of model-derived hydrologic budgets differs from that based on geological salinity estimates. The budgets calculated from the simulations of Marzocchi et al. (2015) never correspond to a sea level drop of 1000 m, but salinity estimates would indicate sea level drops exceeding that value. However, sea-surface salinity estimates for this time period are very uncertain and a 1000 m drop seems less likely to have occurred. Future modelling studies will be able to provide more accurate estimates for the sea level drop in the Black Sea if reliable salinity data for this time period becomes available. This would be useful to test whether the sea level drops calculated from salinity estimates are close (or not) to those derived from hydrologic budgets.

5.2. Did the Caspian sea level drop 1000 m during the Late Miocene?

We can apply our results by deriving the hydrologic budget that would cause the Caspian sea level to go down by 1000 m. As in the previous section, arguing that the connection between the Black Sea and the Caspian Sea was shallow, we study the Caspian Sea separately. Assuming again that E − P was equal or smaller than 1 m/year we find that R has to be lower than about 0.1 m/year (74 km^3/year; Fig. 7c). The required R for a sea level lowering is much smaller than the modern annual mean discharge of the Volga River (247 km^3/year; Overeem et al., 2003). Thus, the Volga or any other river in the Caspian Sea needs to be drastically reduced to acclaim for a large sea level drop. Based on the dimensions of the Volga canyon, it has been proposed that at the time, the discharge of this river was at least as large as it is at present (e.g., Abdullayev et al., 2012). A 1000 m sea level drop and a simultaneous formation of a deep palaeo-Volga canyon would thus seem incompatible.

Our calculations from the Late Miocene climate experiments of Marzocchi et al. (2015) indicate that the hydrologic budget of the Caspian Sea is positive if the Volga River flowed there (Fig. 7c and Figs. 8a, 8b). In this situation overspilling from the Caspian Sea into the Black Sea would have occurred. If the Volga River is excluded from the river discharge into the Caspian Sea the equivalent surface freshwater flux (E − P − R) is close to 0.26 m/year, which is smaller than that of the present-day Mediterranean Sea. This hydrologic budget corresponds to a sea level drop of about 100 m (Fig. 7c), which is within the range proposed by van Baak et al. (in press). In this case, the Volga River would have drained into the Black Sea. Interestingly, the runoff of the Volga River calculated by Marzocchi et al. (2015) is so large that it causes the hydrologic budget of the basin in which it flows, in this case the Black Sea, to become very

positive. Thus, a simultaneous high-magnitude sea level drop in both the Black Sea and the Caspian Sea is not possible (Figs. 7b and 7c). According to van Baak et al. (in press), salinity in the Caspian basin remained relatively stable at 10 g/kg from 5.6 to 5.5 Ma. We find that a sea level fall of 100–150 m would have increased salinity by 4–5 g/kg (from a salinity of 10 to 14–15 g/kg; Fig. 9a), which is probably too small an increase to detect. The possibility of a 1000 m sea level drop at this time can be discarded because it would raise salinity to a value of 47 g/kg, which exceeds by far the brackish conditions inferred by van Baak et al. (in press; Fig. 9a).

When the alternative hypsometric curve is considered, the hydrologic budget calculated from Marzocchi et al. (2015), for the case that the Volga and Danube rivers were not connected to this basin, corresponds to a sea level drop of about 1000 m (Fig. 7f). In the Caspian Sea, due to the small surface area occupied by the deep domains of the basin, R has to be very small to lower the sea level below the shelves. Once this value is reached, even small reductions of R, can have a large impact on the amplitude of the sea level drop. A sea level drop of 1000 m, according to our results, would cause a salinity increase from 10 to a value of 26 g/kg (Fig. 9b). However, van Baak et al. (in press) report no major environmental shifts during this period and estimate a constant salinity of 10 g/kg from 5.6 to 5.5 Ma. A 1000 m sea level drop in the Caspian Sea can be therefore ruled out. This result confirms that the alternative hypsometric curve represents a too extreme basin configuration and that the sea level drop in the Black Sea and the Caspian Sea may have been smaller than that inferred from this curve. More detailed information regarding the configuration of the continental slope of the Caspian Sea would allow future modelling studies to reconstruct more precisely the sea level drop in this basin.

To summarise, by combining salinity estimates derived from field observations and Late Miocene hydrologic budgets we are able to discard a 1000 m sea level drop in the Caspian Sea from 5.6 to 5.5 Ma. For an isolated Caspian Sea, a drop in sea level below the shelves can only occur if the Volga River did not flow there.

5.3. Further implications

So far in this discussion, we have studied each of the basins in isolation arguing that the connection between the Black Sea and the Caspian Sea was shallow (Popov et al., 2006). We now use our analysis to look into the possibility that the Black Sea and the Caspian Sea remained connected during this time interval. This scenario necessarily requires the connection between the Mediterranean Sea and the Paratethys to be shallower than the channel between the Black Sea and the Caspian Sea (Fig. 8d). For the Paratethys as a whole, the model results derived from the simulations of Marzocchi et al. (2015) predict a positive hydrologic budget, which is close to neutral (Fig. 7a and d). Any drop in excess of the level of the sill between the Paratethys and the Mediterranean Sea would thus seem unlikely and the Black Sea and the Caspian Sea would remain connected (Figs. 7a, d and 8d). In other words, if the Paratethys sea level drop induced by the Mediterranean level lowering is not enough to isolate the basins, further sea level drop would not occur.

If this was the case and both basins remained connected, one would expect a similar salinity evolution in the Black Sea and the Caspian Sea over time. Unfortunately, a comparison between the available salinity data-sets for these basins is not straightforward. In the Caspian Sea a generic average salinity of the basin is reconstructed from the study of ostracods (van Baak et al., in press). In the Black Sea, diatoms are used to estimate the sea-surface salinity (Schrader, 1978; van Baak et al., 2015), which is more prone to fluctuate due to air-sea interactions and local processes. To test this hypothesis, reliable and comparable salinity data for the Late Miocene Black Sea and the Caspian Sea is required.

5.4. Comparison to an isolated Mediterranean Sea

Previous quantitative analyses have focused on the response of the sea level of the Mediterranean when it gets isolated from the Atlantic Ocean (Blanc, 2000; Meijer and Krijgsman, 2005). Using a Late Miocene bathymetry, Meijer and Krijgsman (2005) found that with the modern Mediterranean hydrologic budget, closure would cause the Mediterranean sea level to drop more than 2000 m. In the Late Miocene Black Sea and Caspian Sea, the hydrologic budgets should be very different from the modern ones to achieve a 1000 m (or more) sea level drop (Fig. 7). This requires E − P to dramatically increase and/or R to decrease. As commented in Section 5.1, modelling and palynological studies do not indicate abnormally dry conditions over the Mediterranean Sea or Paratethys during the Late Miocene (Gladstone et al., 2007; Popescu et al., 2010; Christeleit et al., 2015; Marzocchi et al., 2015). As to R, global climate model simulations from Marzocchi et al. (2015) indicate that the river discharge (i.e., total volume) into the Late Miocene Black Sea and Caspian Sea was, respectively, larger than it is today. We thus propose that if a large sea level drop occurred in one of the Paratethys sub-basins, it was most likely caused by a rearrangement of the drainage system. In particular, a sea level drop would be possible in the case that none of the large Paratethyan Rivers (Volga and Danube) drained into a basin (Fig. 7).

As in the Paratethys, Mediterranean average salinity only shows important deviations from the initial salinity of the basin when the sea level drop is large (Meijer and Krijgsman, 2005). Time to equilibrium is found to be shorter than a precession cycle in the Mediterranean Sea (Meijer and Krijgsman, 2005). This is also the case in the Paratethys, with the exception of the case where both E − P and R are very small (Fig. 5).

6. Conclusions

We have shown that a relatively simple analysis provides valuable quantitative constraints on the sensitivity of sea level of the Paratethys sub-basins to the hydrologic budget. The model approach allows us to study sea level fall and salinity change in a consistent way and provides a framework to interpret the spatially limited observations on the scale of entire (sub-)basins. The following conclusions have been reached independent of geological data:

- In the Caspian Sea, the river discharge required for a sea level drop below the shelves is smaller than in the Black Sea.
- Basin salinity only starts to rise significantly for sea level drops below the shelves.
- For a given basin, time to equilibrium is typically not longer than 10 kyr. When E − P and R are small, time to equilibrium is longer, but it never reaches 100 kyr.
- Climate-model derived hydrologic budgets indicate that the Volga River renders the hydrologic budget of the basin in which it terminates very positive. A sea level drop below the shelves at the same time in the Black Sea and the Caspian Sea thus seems unlikely.

Combining our model analysis with the available geological data, two further conclusions can be drawn, regarding the possibility of a large sea level fall from 5.6 to 5.5 Ma:

- A 1000 m sea level drop in the Black Sea can be ruled out based on the Late Miocene hydrologic budgets calculated from the simulations of Marzocchi et al. (2015). Salinity reconstructions, although very uncertain, would leave this possibility open. In our calculations, even excluding the Volga and the Danube rivers from the discharge into the Black Sea proves not to be enough to lower the Black sea level by 1000 m.
- A sea level drop in the Caspian Sea of 1000 m or more, is unlikely. The Caspian sea level only drops below its shelves if the Volga

River is absent or much smaller than it is at present. A large sea level drop coeval with the formation of an extensive, deeply incising Volga canyon is unlikely.

Supplementary data to this article can be found online at http://dx.doi.org/10.1016/j.margeo.2016.05.002.

Acknowledgments

This research is funded by NWO/ALW (820.01.021) and computational resources were provided by the Netherlands Research Center for Integrated Solid Earth Science (ISES 3.2.5. High End Scientific Computational Resources). We thank Rinus Wortel, Dirk Simon, Robin Topper and Wout Krijgsman for valuable discussions and suggestions to improve the manuscript. We thank Gabor Tari and an anonymous referee for their insightful comments on our work. We are also grateful to the editor Edward Anthony for his handling of the manuscript.

References

Abdullayev, N.R., Riley, G.W., Bowman, A.P., 2012. Regional controls on lacustrine sandstone reservoirs: the Pliocene of the South Caspian basin. In: Baganz, O.W., Bartov, Y., Bohacs, K., Nummedal, D. (Eds.), Lacustrine Sandstone Reservoirs and Hydrocarbon Systems, pp. 71–98.

Alekseev, A.S., Sorokin, V.M., Sokolov, V.N., Kuprin, P.N., 2012. A *Calciosolenia brasiliensis* (Coccolithophorida) find in neogene sediments of a deep Black Sea basin and its connection with the Mediterranean. Dokl. Earth Sci. 446 (2), 1148–1150. http://dx.doi.org/10.1134/S1028334X12100066.

Badertscher, S., Fleitmann, D., Cheng, H., Edwards, R.L., Göktürk, O.M., Zumbühl, A., Leuenberger, M., Tüysüz, O., 2011. Pleistocene water intrusions from the Mediterranean and Caspian seas into the Black Sea. Nat. Geosci. 4 (4), 236–239. http://dx.doi.org/10.1038/ngeo1106.

Blanc, P.-L., 2000. Of sills and straits: a quantitative assessment of the Messinian Salinity Crisis. Deep-Sea Res. 47, 1429–1460. http://dx.doi.org/10.1016/S0967-0637(99)00113-2.

Christeleit, E.C., Brandon, M.T., Zhuang, G., 2015. Evidence for deep-water deposition of abyssal Mediterranean evaporites during the Messinian salinity crisis. Earth Planet. Sc. Lett. 427, 226–235. http://dx.doi.org/10.1016/j.epsl.2015.06.060.

Clauzon, G., Suc, J.P., Gautier, F., Berger, A., Loutre, M.F., 1996. Alternate interpretation of the Messinian salinity crisis: controversy resolved? Geology 24 (4), 363–366. http://dx.doi.org/10.1130/0091-7613(1996)024<0363:AIOTMS>2.3.CO;2.

Clauzon, G., Suc, J.P., Popescu, S.-M., Marunteanu, M., Rubino, J.L., Marinescu, F., Melinte, M.C., 2005. Influence of Mediterranean sea-level changes on the Dacic Basin (Eastern Paratethys) during the late Neogene: the Mediterranean Lago Mare facies deciphered. Basin Res. 17 (3), 437–462. http://dx.doi.org/10.1111/j.1365-2117.2005.00269.x.

Farr, T.G., Kobrick, M., 2000. Shuttle Radar Topography Mission produces a wealth of data. EOS Trans. Am. Geophys. Union 81, 583–585.

Garnier, J., Billen, G., Hannon, E., Fonbonne, S., Videnina, Y., Soulie, M., 2002. Modelling the transfer and retention of nutrients in the drainage network of the Danube River. Estuar. Coast. Shelf Sci. 54 (3), 285–308. http://dx.doi.org/10.1006/ecss.2000.0648.

Gheorghian, M., 1978. Micropaleontological investigations of the sediments from sites 379, 380, and 381 of leg 42B. In: Ross, D.A., Neprochnov, Y.P. (Eds.), Init. Rep. Deep Sea Drill. Proj. vol. 42, part 2. U.S. Government Printing Office, Washington, D.C., pp. 783–787

Gillet, H., Lericolais, G., Rehault, J.P., Dinu, C., 2003. La stratigraphie oligo-miocène et la surface d'érosion messinienne en mer Noire, stratigraphie sismique haute resolution. Compt. Rendus Geosci. 335 (12), 907–916. http://dx.doi.org/10.1016/j.crte.2003.08.008.

Gillet, H., Lericolais, G., Réhault, J.P., 2007. Messinian event in the Black Sea: evidence of a Messinian erosional surface. Mar. Geol. 244 (1), 142–165. http://dx.doi.org/10.1016/j.margeo.2007.06.004.

Gladstone, R., Flecker, R., Valdes, P., Lunt, D., Markwick, P., 2007. The Mediterranean hydrologic budget from a Late Miocene global climate simulation. Palaeogeogr. Palaeoclimatol. Palaeoecol. 251 (2), 254–267. http://dx.doi.org/10.1016/j.palaeo.2007.03.050.

Green, T., Abdullayev, N., Hossack, J., Riley, G., Roberts, A.M., 2009. Sedimentation and subsidence in the south Caspian Basin, Azerbaijan. Geol. Soc. Spec. Pub. 312 (1), 241–260. http://dx.doi.org/10.1144/SP312.12.

Grothe, A., Sangiorgi, F., Mulders, Y.R., Vasiliev, I., Reichart, G.-J., Brinkhuis, H., Stoica, M., Krijgsman, W., 2014. Black Sea desiccation during the Messinian Salinity Crisis: fact or fiction? Geology 42 (7), 563–566. http://dx.doi.org/10.1130/G35503.1.

Hsü, K.J., Giovanoli, F., 1979. Messinian event in the Black Sea. Palaeogeogr. Palaeoclimatol. Palaeoecol. 29, 75–93. http://dx.doi.org/10.1016/0031-0182(79)90075-0.

Hsü, K.J., Ryan, W.B.F., Cita, M.B., 1973. Late Miocene desiccation of the Mediterranean. Nature 242 (5395), 240–244.

Jauzein, A., Hubert, P., 1984. Les bassins oscillants: Un modèle de genèse des séries salines. B. Sci. Géol. 37 (3), 267–282.

Jones, R.W., Simmons, M.D., 1996. A review of the stratigraphy of eastern Paratethys (Oligocene-Holocene). Bull. Br. Mus. Nat. Hist. Geol. 52, 25–50.

Jousé, A.P., Mukhina, V.V., 1978. Diatom units and the paleogeography of the Black Sea in the late Cenozoic (DSDP, Leg 42B). In: Ross, D.A., Neprochnov, Y.P. (Eds.), Init. Rep. Deep Sea Drill. Proj. vol. 42, part 2. U.S. Government Printing Office, Washington, D.C., pp. 903–950

Kojumdgieva, E., 1979. Critical notes on the stratigraphy of Black Sea boreholes (Deep Sea Drilling Project, Leg 42B). Geol. Balcanica 9, 107–110.

Krijgsman, W., Hilgen, F.J., Raffi, I., Sierro, F.J., Wilson, D.S., 1999. Chronology, causes and progression of the Messinian salinity crisis. Nature 400 (6745), 652–655. http://dx.doi.org/10.1038/23231.

Krijgsman, W., Stoica, M., Vasiliev, I., Popov, V.V., 2010. Rise and fall of the Paratethys Sea during the Messinian Salinity Crisis. Earth Planet. Sc. Lett. 290 (1), 183–191. http://dx.doi.org/10.1016/j.epsl.2009.12.020.

Kroonenberg, S.B., Simmons, M.D., Alekseevski, N.I., Aliyeva, E., Allen, M.B., Aybulatov, D.N., Baba-Zadeh, A., Babyukova, E.N., Davies, C.E., Hinds, D.J., Hoogendoorn, R.M., Huseynov, D., Ibrahimov, B., Mamedov, P., Overeem, I., Rusakov, G.V., Suleymanova, S.F., Svitoch, A.A., Vincent, S.J., 2005. Two deltas, two basins, one river, one sea: the modern Volga delta as an analogue of the Neogene Productive Series, South Caspian Basin. In: Giosan, L., Bhattacharya, J.P. (Eds.), SEPM Spec. Publ., River Deltas - Concepts, Models and Examples. SEPM, Tulsa, Oklahoma, U.S.A., pp. 231–256.

Leever, K.A., Matenco, L., Rabagia, T., Cloetingh, S., Krijgsman, W., Stoica, M., 2010. Messinian sea level fall in the Dacic Basin (Eastern Paratethys): palaeogeographical implications from seismic sequence stratigraphy. Terra Nova 22 (1), 12–17. http://dx.doi.org/10.1111/j.1365-3121.2009.00910.x.

Manzi, V., Gennari, R., Hilgen, F., Krijgsman, W., Lugli, S., Roveri, M., Sierro, F.J., 2013. Age refinement of the Messinian salinity crisis onset in the Mediterranean. Terra Nova 25 (4), 315–322. http://dx.doi.org/10.1111/ter.12038.

Mariotti, A., Struglia, M.V., Zeng, N., Lau, K.-M., 2002. The hydrological cycle in the Mediterranean region and implications for the water budget of the Mediterranean Sea. J. Clim. 15 (13), 1674–1690. http://dx.doi.org/10.1175/1520 0442(2002)015<1674:THCITM>2.0.CO;2.

Marzocchi, A., Lunt, D.J., Flecker, R., Bradshaw, C.D., Farnsworth, A., Hilgen, F.J., 2015. Orbital control on late Miocene climate and the North African monsoon: insight from an ensemble of sub-precessional simulations. Clim. Past 11, 1271–1295. http://dx.doi.org/10.5194/cp-11-1271-2015.

Meijer, P.T., Krijgsman, W., 2005. A quantitative analysis of the desiccation and re-filling of the Mediterranean during the Messinian Salinity Crisis. Earth Planet. Sc. Lett. 240 (2), 510–520. http://dx.doi.org/10.1016/j.epsl.2005.09.029.

Munteanu, I., Matenco, L., Dinu, C., Cloetingh, S., 2012. Effects of large sea-level variations in connected basins: the Dacian–Black Sea system of the Eastern Paratethys. Basin Res. 24 (5), 583–597. http://dx.doi.org/10.1111/j.1365-2117.2012.00541.x.

Overeem, I., Veldkamp, A., Tebbens, L., Kroonenberg, S.B., 2003. Modelling Holocene stratigraphy and depocentre migration of the Volga delta due to Caspian Sea-level change. Sediment. Geol. 159 (3), 159–175. http://dx.doi.org/10.1016/S0037-0738(02)00256-7.

Ozyavas, A., Khan, S.D., Casey, J.F., 2010. A possible connection of Caspian Sea level fluctuations with meteorological factors and seismicity. Earth Planet. Sc. Lett. 299 (1), 150–158. http://dx.doi.org/10.1016/j.epsl.2010.08.030.

Popescu, S.-M., 2006. Late Miocene and early Pliocene environments in the southwestern Black Sea region from high-resolution palynology of DSDP Site 380A (Leg 42B). Palaeogeogr. Palaeoclimatol. Palaeoecol. 238 (1), 64–77. http://dx.doi.org/10.1016/j.palaeo.2006.03.018.

Popescu, S.-M., Biltekin, D., Winter, H., Suc, J.-P., Melinte-Dobrinescu, M.C., Klotz, S., Combourieu-Nebout, N., Rabineau, M., Clauzon, G., Deaconu, F., 2010. Pliocene and Lower Pleistocene vegetation and climate changes at the European scale: long pollen records and climatostratigraphy. Quat. Int. 219, 152–167. http://dx.doi.org/10.1016/j.quaint.2010.03.013.

Popov, S.V., Rögl, F., Rozanov, A.Y., Steiniger, F.F., Shcherba, I.G., Kovac, M., 2004. Lithological-Paleogeographic Maps of Paratethys: 10 Maps Late Eocene to Pliocene. Courier Forschungsinstitut Senckenberg, Frankfurt/Main.

Popov, S.V., Shcherba, I.G., Ilyina, L.B., Nevesskaya, L.A., Paramonova, N.P., Khondkarian, S.O., Magyar, I., 2006. Late Miocene to Pliocene palaeogeography of the Paratethys and its relation to the Mediterranean. Palaeogeogr. Palaeoclimatol. Palaeoecol. 238 (1), 91–106. http://dx.doi.org/10.1016/j.palaeo.2006.03.020.

Radionova, E., Golovina, L., 2011. Upper Maeotian-Lower Pontian "Transitional Strata" in the Taman Peninsula: stratigraphic position and paleogeographic interpretation. Geol. Carpath. 62 (1), 77–90. http://dx.doi.org/10.2478/v10096-011-0007-x.

Rögl, F., 1996. Stratigraphic correlation of the Paratethys Oligocene and Miocene. Mitt. Gesell. Geol. Bergb. Österr. 41, 65–73.

Rögl, F., 1999. Mediterranean and Paratethys. Facts and hypotheses of an Oligocene to Miocene paleogeography (short overview). Geol. Carpath. 50 (4), 339–349.

Ross, D.A., Neprochnov, Y.P., Hsü, K.J., Stoffers, P., Supko, P., Trimonis, E.S., Percival, S.F., Erickson, A.J., Degens, E.T., Hunt, J.M., Manheim, F.T., Senalp, M., Traverse, A., 1978. Init. Rep. Deep Sea Drill. Proj. vol. 42, part 2. U.S. Government Printing Office, Washington, D. C. http://dx.doi.org/10.2973/dsdp.proc.42-2.1978.

Roveri, M., Flecker, R., Krijgsman, W., Lofi, J., Lugli, S., Manzi, V., Sierro, F.J., Bertini, A., Camerlenghi, A., De Lange, G., Govers, R., Hilgen, F.G., Hübscher, C., Meijer, P.T., Stoica, M., 2014a. The Messinian Salinity Crisis: past and future of a great challenge for marine sciences. Mar. Geol. 352, 25–58. http://dx.doi.org/10.1016/j.margeo.2014.02.002.

Roveri, M., Manzi, V., Bergamasco, A., Falcieri, F.M., Gennari, R., Lugli, S., Schreiber, B.C., 2014b. Dense shelf water cascading and Messinian canyons: a new scenario for the Mediterranean salinity crisis. Am. J. Sci. 314 (3), 751–784. http://dx.doi.org/10.2475/05.2014.03.

Salhotra, A.M., Adams, E.E., Harleman, D.R.F., 1985. Effect of salinity and ionic composition on evaporation: analysis of Dead Sea evaporation pans. Water Resour. Res. 21 (9), 1336–1344. http://dx.doi.org/10.1029/WR021i009p01336.

Schrader, H.-J., 1978. Quaternary through Neogene history of the Black Sea, deduced from the paleoecology of diatoms, silicoflagellates, ebridians, and chrysomonads. In: Ross, D.A., Neprochnov, Y.P. (Eds.), Init. Rep. Deep Sea Drill. Proj. vol. 42, part 2. U.S. Government Printing Office, Washington, D.C., pp. 789–901

Staneva, J.V., Dietrich, D.E., Stanev, E.V., Bowman, M.J., 2001. Rim current and coastal eddy mechanisms in an eddy-resolving Black Sea general circulation model. J. Mar. Syst. 31 (1), 137–157. http://dx.doi.org/10.1016/S0924-7963(01)00050-1.

Stoica, M., Lazăr, I., Krijgsman, W., Vasiliev, I., Jipa, D., Floroiu, A., 2013. Paleoenvironmental evolution of the East Carpathian foredeep during the late Miocene–early Pliocene (Dacian Basin; Romania). Glob. Planet. Chang. 103, 135–148. http://dx.doi.org/10.1016/j.gloplacha.2012.04.004.

Suc, J.P., Do Couto, D., Melinte-Dobrinescu, M.C., Macalet, R., Quillévéré, F., Clauzon, G., Csato, I., Rubino, J.-L., Popescu, S.-M., 2011. The Messinian Salinity Crisis in the Dacic Basin (SW Romania) and early Zanclean Mediterranean–eastern Paratethys high sea-level connection. Palaeogeogr. Palaeoclimatol. Palaeoecol. 310 (3), 256–272. http://dx.doi.org/10.1016/j.palaeo.2011.07.018.

Tari, G., Fallah, M., Kosi, W., Floodpage, J., Baur, J., Bati, Z., Sipahioğlu, N.O., 2015. Is the impact of the Messinian Salinity Crisis in the Black Sea comparable to that of the Mediterranean? Mar. Pet. Geol. 66 (1), 135–148. http://dx.doi.org/10.1016/j.marpetgeo.2015.03.021.

Thunell, R.C., Locke, S.M., Williams, D.F., 1988. Glacio-eustatic sea-level control on Red Sea salinity. Nature 334, 601–604. http://dx.doi.org/10.1038/334601a0.

Topper, R.P.M., Meijer, P.T., 2013. A modeling perspective on spatial and temporal variations in Messinian evaporite deposits. Mar. Geol. 336, 44–60. http://dx.doi.org/10.1016/j.margeo.2012.11.009.

Ünlülata, Ü., Oğuz, T., Latif, M.A., Özsoy, E., 1990. On the physical oceanography of the Turkish Straits. In: Pratt, L.J. (Ed.), The Physical Oceanography of Sea Straits. Springer, Netherlands, pp. 25–60 http://dx.doi.org/10.1007/978-94-009-0677-8_2.

van Baak, C.G.C., Radionova, E.P., Golovina, L.A., Raffi, I., Kuiper, K.F., Vasiliev, I., Krijgsman, W., 2015. Messinian events in the Black Sea. Terra Nova 27 (6), 433–441. http://dx.doi.org/10.1111/ter.12177.

van Baak, C. G. C., Stoica, M., Grothe, A., Aliyeva, E., Krijgsman, W.,2016 Mediterranean-Paratethys Connectivity during the Messinian Salinity Crisis: The Pontian of Azerbaijan, doi: http://dx.doi.org/10.1016/j.gloplacha.2016.04.005 (in press).

Vasiliev, I., Krijgsman, W., Stoica, M., Langereis, C.G., 2005. Mio-Pliocene magnetostratigraphy in the southern Carpathian foredeep and Mediterranean–Paratethys correlations. Terra Nova 17 (4), 376–384. http://dx.doi.org/10.1111/j.1365-3121.2005.00624.x.

Vasiliev, I., Reichart, G.-J., Krijgsman, W., 2013. Impact of the Messinian Salinity Crisis on Black Sea hydrology—insights from hydrogen isotopes analysis on biomarkers. Earth Planet. Sc. Lett. 362, 272–282. http://dx.doi.org/10.1016/j.epsl.2012.11.038.nzi.

Vasiliev, I., Reichart, G.-J., Grothe, A., Sinninghe Damsté, J.S., Krijgsman, W., Sangiorgi, F., Weijers, J.W.H., van Roij, L., 2015. Recurrent phases of drought in the upper Miocene of the Black Sea region. Palaeogeogr. Palaeoclimatol. Palaeoecol. 423, 18–31. http://dx.doi.org/10.1016/j.palaeo.2015.01.020.

Warren, J.K., 2006. Evaporites: Sediments, Resources, and Hydrocarbons. Springer-Verlag, New York.

Zubakov, V.A., 1988. Climatostratigraphic scheme of the Black Sea Pleistocene and its correlation with the oxygen-isotope scale and glacial events. Quat. Res. 29, 1–24. http://dx.doi.org/10.1016/0033-5894(88)90067-1.

Further reading

Markwick, P., 2007. The palaeogeographic and palaeoclimatic significance of climate proxies for data-model comparisons. In: Williams, M., Haywood, A.M., Gregory, F.J., Schmidt, D.N. (Eds.), Deep-Time Perspectives on Climate Change: Marrying the Signal from Computer Models and Biological ProxiesThe Micropalaeontology Society, Sp. Publication. The Geological Society, London, pp. 251–312.